NIST-NPL Interlaboratory Pulse Measurement Comparison

N. G. Paulter, Andrew J. A. Smith, D. R. Larson, *Senior Member, IEEE*, T. M. Souders, and Alan G. Roddie

***Abstract*—A comparison of the pulse parameter values obtained from the pulse measurement services of the National Institute of Standards and Technology, USA, and the National Physical Laboratory, U.K., was performed. The comparison was based on the pulse parameters of amplitude, transition duration, overshoot, and undershoot (preshoot). The parameter comparison was applied to raw (measured) waveforms, corrected waveforms (if applicable), and reconstructed waveforms. The results of the comparison show that the pulse parameter values for both national laboratories are within published uncertainties.**

***Index Terms*—Interlaboratory comparison, overshoot, pulse amplitude, pulse parameters, pulse waveforms, transition duration, undershoot.**

I. Introduction

THE National Physical Laboratory (NPL) in the U.K. and the National Institute of Standards and Technology (NIST) in the USA provide measurement services for pulse parameters of high-speed (transition duration $\leq$ 350-ps pulse generators [1], [2]). Clients that use NIST's and the NPL's pulse measurement service include the aerospace, telecommunications, test equipment, and computer industries.

The purpose for the work presented herein is to provide a comparison of the pulse measurement services of the two national laboratories. The pulse parameters reported to the customer, and that are common to both NPL and NIST, are pulse amplitude and pulse transition duration (also known as rise time or fall time). Therefore, these two pulse parameters are used in the comparison. In addition, the pulse parameters of overshoot and undershoot (preshoot) are compared although neither NIST or NPL presently report these parameters routinely to their customers. NIST and NPL have recently completed an uncertainty analysis for overshoot and undershoot measurements and will be providing values for these parameters in their measurement service in 2002.

The comparison was done using the pulse parameter values computed for the raw waveforms and also for each waveform generated in the subsequent waveform processing procedure. Several comparisons were done with the reconstructed waveforms to identify if discrepancies occur either because of differences in the processing algorithms or because of errors in the estimates of the sampler impulse response. Also, to ensure that the pulse parameter extraction software did not introduce anomalies into results, the NPL and NIST pulse parameter extraction software was also tested. In this paper, we will first describe the pulse parameter measurement process, which includes acquiring a waveform, correcting the waveform, and reconstructing the waveform; and then present the results of the comparison.

Manuscript received June 3, 2002; revised July 7, 2003.

N. G. Paulter and D. R. Larson are with the Electricity Division, National Institute of Standards and Technology, Gaithersburg, MD 20899 USA.

A. J. A. Smith and A. G. Roddie are with the Centre for Electromagnetic and Time Metrology, Middlesex, U.K.

T. M. Souders, retired, was with the Electricity Division, NIST, 100 Bureau Drive, Gaithersburg, MD 20899 USA.

Digital Object Identifier 10.1109/TIM.2003.820456

II. Background

The process of extracting pulse parameters starts with measuring the pulse (which yields the measured waveform), possibly correcting the waveform for any gain and timebase errors caused by the sampler, correcting for effects that the sampler impulse response and jitter have on the waveform (the waveform reconstruction process), and finally extracting the pulse parameters from the reconstructed waveform. The high-speed pulses were measured using digitizing equivalent-time sampling oscilloscopes (herein called samplers) having 3-dB attenuation bandwidths of approximately 20 GHz (presently, both NIST and NPL use 50-GHz samplers in their measurement service but at the time this comparison was being performed NIST was using 20-GHz samplers). Waveforms were acquired with the samplers and transferred to a computer for processing. Whether or not a correction is performed for gain errors and time-base errors is based on the ability to distinguish between the pulse parameter error and the published parameter uncertainty [1], [2].

The last step in obtaining a waveform from which the pulse parameters are extracted is to perform a reconstruction. The reconstruction is necessary because the impulse response of the sampler distorts the pulse waveform features relative to that of the input pulse. However, because only an estimate for the sampler impulse response is available [3]–[5], the reconstructed waveform is only an estimate of the input pulse. NIST and NPL used regularized reconstruction methods, using a method similar to that described in [3], in this comparison to obtain waveforms that are estimates of the input pulses. Both national laboratories are presently working on methods to improve the accuracy of the sampler impulse response estimate that, in turn, would decrease the pulse parameter uncertainty contribution from the sampler impulse response [6]–[10].

III. Comparison Results

A pulse generator (nominal specifications: 15-ps transition duration, 0.25-V pulse amplitude, and 0.1% settling in $<$2 ns) and trigger system [11] were shipped between the two national laboratories to minimize any potential differences that may be

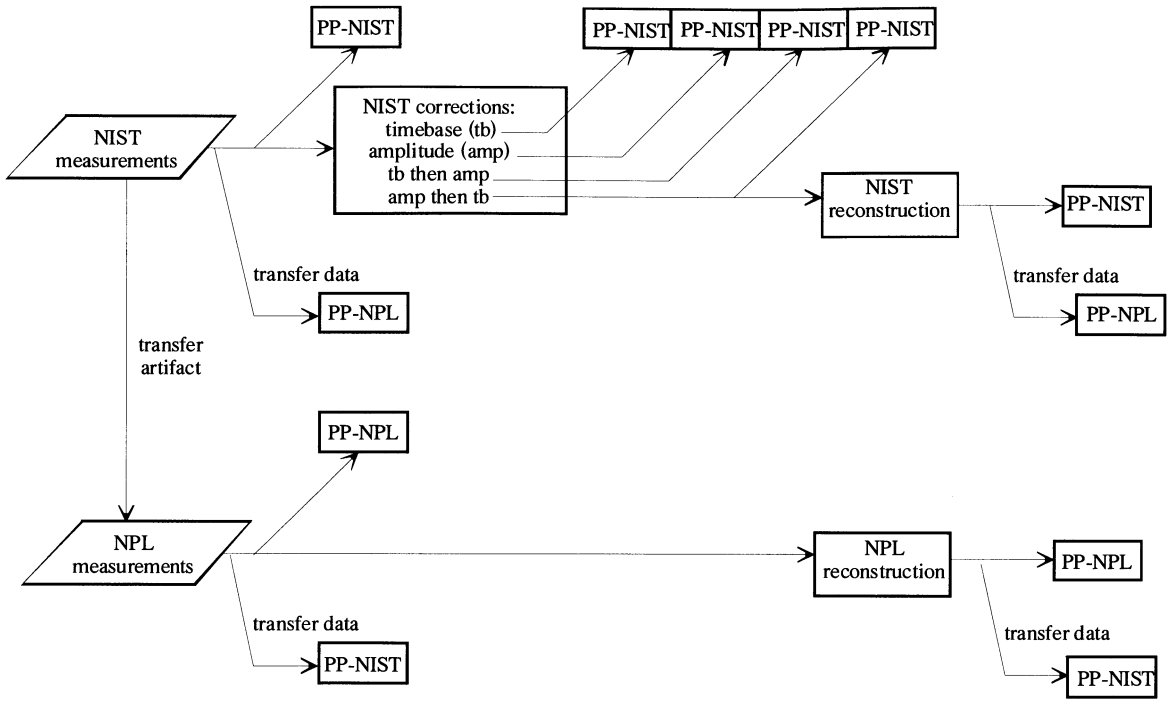

Fig. 1. NPL-NIST interlaboratory comparison flowchart. "PP-NIST" and "PP-NPL" indicate whether NIST or NPL pulse parameter algorithms were used.

caused by using distinct pulse generators or trigger systems. The room temperature of the laboratories were not the same during the measurements: NPL laboratory temperature was typically 21 °C±2 °C, whereas that of NIST was 23 °C±1 °C. Fig. 1 shows a flowchart depicting the NPL-NIST interlaboratory pulse parameter comparison.

A. Measured Waveforms and Pulse Parameter Extraction Software

The waveforms were measured using a specific manufacturer's 20-GHz sampling oscilloscopes because both national laboratories had these samplers in their inventory. The raw waveforms used in this comparison are shown in Fig. 2. Both NIST's and NPL's pulse parameter extraction software are based on histogram methods [12], [13]. The acquired waveforms are step-like waveforms and, therefore, have a bimodal amplitude distribution: one mode corresponds to state 2 (S_2, the top level in this case) and the other to state 1 (S_1, the bottom level in this case). S_2 and S_1 are the values of the nominally constant-valued regions on either side of the transition in a step-like (or two-state) waveform. The histogram size (number of histogram bins) is found using laboratory-specific criteria, such as a minimum number of elements counted in the smaller of the two mode bins (presently used by NIST), or a fixed number of histogram bins (typically 2^n, where n is an integer) (presently used by NPL), or by an optimal search (proposed NIST method) [14]. The difference between S_2 and S_1 is the pulse amplitude [13], [15]. The transition duration is defined as the difference between the instants when the waveform crosses two different reference levels. The 10% and 90% reference levels are typically used to define the transition duration, the percentage referring to the pulse amplitude. Occasionally these levels are ill-defined for a particular waveform shape in which case the 20% and 80% reference levels may be used to determine the transition duration.

Figs. 3–6 show pulse parameter extraction results for the NIST and NPL algorithms and for different positions of the transition within the epoch of the waveforms shown in Fig. 2. The horizontal-axis annotation, "Measurement Method," indicates the pulse parameter extraction algorithm and waveform length.

A. NIST algorithm, 2^n number of histogram bins, full waveform (1024 elements).
B. NIST algorithm, 2^n number of histogram bins, truncated waveform.
C. NIST algorithm, variable number of histogram bins, full waveform.
D. NIST algorithm, variable number of histogram bins, truncated waveform.
E. NPL algorithm, 2048 histogram bins, full waveform.
F. NPL algorithm, 4096 histogram bins, full waveform.

Methods A to D were applied to all nine waveforms. Method E was applied to all four NIST waveforms and two NPL waveforms and Method F applied to one NIST waveform and one NPL waveform. Methods E and F were not applied to NPL-1 and -2 because these waveforms were used to examine the effect of position on the values of the pulse parameters, which was determined by Methods A to D.

The waveform length was truncated in Methods B and D so that all waveforms had approximately the same number of points on either side of the transition. The key in Figs. 3–6 represents the different waveforms (shown in Fig. 2). All waveforms contained 1024 elements (sampled data). The NIST-measured waveforms are the result of 1024 averages whereas the NPL data are the result of 128 averages; all averaging is done internally by

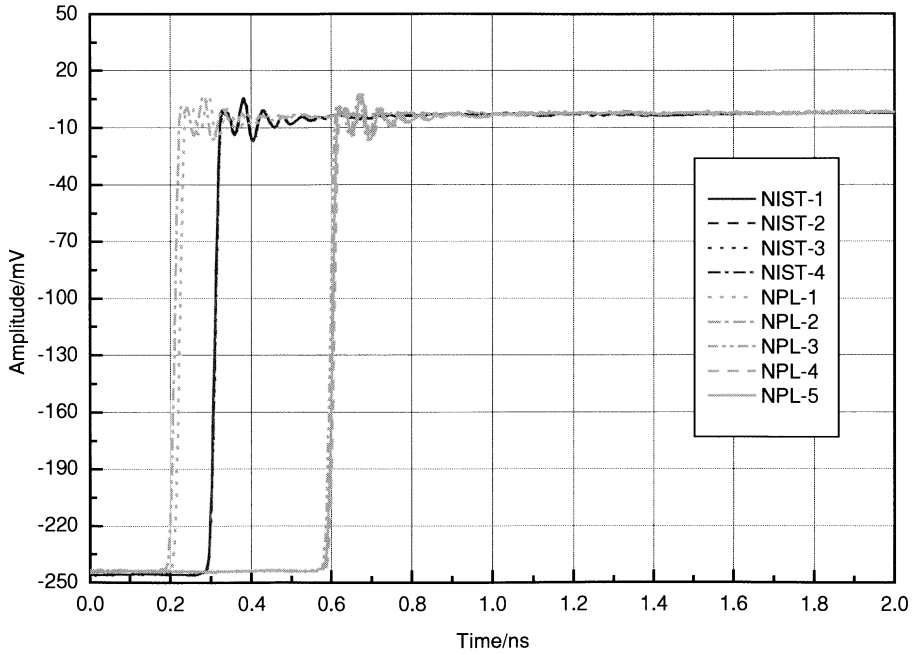

Fig. 2. Plot of the waveforms used in the comparison. The waveforms labeled "NIST" were measured by NIST and the ones labeled "NPL" were measured by NPL. Each waveform was obtained from an independent measurement. The NIST waveforms are virtually overlapping and are the central group (with the transition occurring around 300 ps). NPL-l and -2 are located together and occur around 200 ps. NPL-3, -4, and -5 occur around 600 ps.

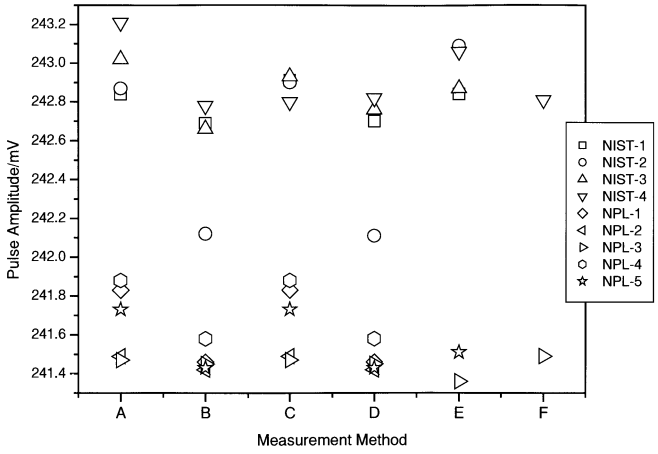

Fig. 3. Signal amplitude of the measured waveforms obtained using different pulse parameter measurement methods A to F (explained in Section III-A of the text). The key represents the nine different waveforms for which the pulse parameters were measured. Methods A to D have been applied to all nine waveforms, Method E to six waveforms, and Method F to two waveforms (see explanation in Section III-A).

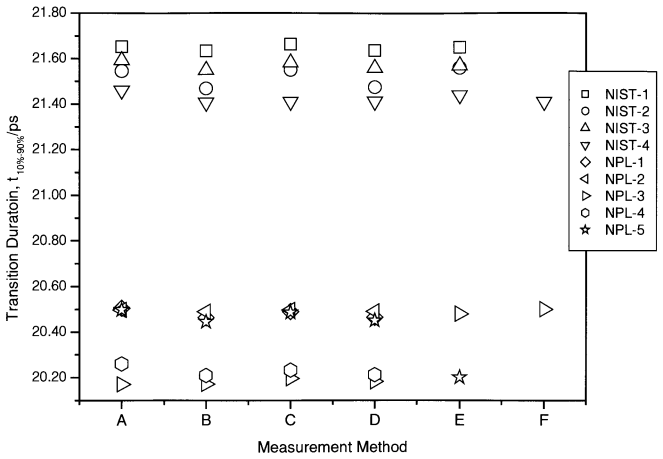

Fig. 4. Transition duration of the measured waveforms obtained using different pulse parameter measurement methods A to F (explained in Section III-A of the text). The key represents the nine different waveforms for which the pulse parameters were measured. Methods A to D have been applied to all nine waveforms, Method E to six waveforms, and Method F to two waveforms (see explanation in Section III-A).

the samplers. There was no observable drift in the waveforms for the time required to acquire the averaged waveforms. The waveforms used in this section represent as-measured data.

Fig. 3 shows the effect of the pulse parameter extraction method, transition location, and waveform truncation on pulse amplitude. For this data, we observed a correlation between the extracted pulse amplitude and the position of the transition within the epoch. This correlation is a result of the fact that S_2 and S_1 are derived from the modes of the histogram and these modes may be affected by the length of the nominally constant-valued regions on either side of the transition. The histogram modes may be affected if the regions are not absolutely constant and are shortened or lengthened. The effect of transition position on S_2 can be observed by comparing Methods A and B and Methods C and D in Fig. 7 for the NIST waveforms. The effect of transition position is effectively the same as waveform truncation and its effect on pulse amplitude, through its effects on S_2 is also shown in Fig. 7. The effect of transition location and truncation will manifest itself in all the other pulse parameters because they are all calculated from pulse amplitude. There also appears to be a slight difference between the pulse parameter values that were extracted using the NIST and NPL algorithms for certain nontruncated waveforms. For pulse amplitude, however, the difference between NIST and NPL reported values is less than 1% of pulse amplitude,

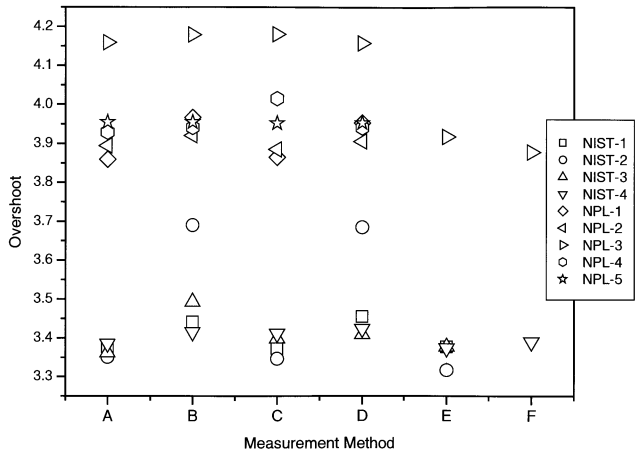

Fig. 5. Percentage overshoot of the measured waveforms obtained using different pulse parameter measurement methods A to F (explained in Section III-A of the text). The key represents the nine different waveforms for which the pulse parameters were measured. Methods A to D have been applied to all nine waveforms. Method E to six waveforms, and Method F to two waveforms (Ssee explanation in Section III-A).

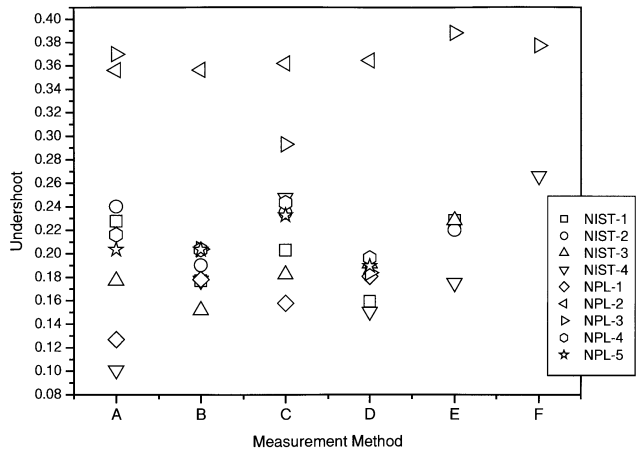

Fig. 6. Percentage undershoot of the measured waveforms obtained using different pulse parameter measurement methods A to F (explained in Section III-A of the text). The key represents the nine different waveforms for which the pulse parameters were measured, Methods A to D have been applied to all nine waveforms, Method E to six waveforms, and Method F to two waveforms (see explanation in Section III-A).

which is less than the reported uncertainties of approximately 1.3% of pulse amplitude.

The difference in pulse amplitude shown in Fig. 3 may be also be the result of different measurement temperatures, different histogram sizes, or the fact that different samplers behave differently. In [16], temperature coefficients for pulse amplitude of up to approximately 1.5 mV/°C are reported. The effect of different histogram sizes on pulse amplitude, which is about 0.15% of pulse amplitude or less, is exhibited by differences between the pulse amplitude values calculated using Methods E and F and Methods A and C.

For calculating percentage post-transition overshoot (hereafter referred to as overshoot) and pre-transition undershoot/preshoot (hereafter referred to as undershoot) values (see Figs. 5 and 6), NIST and NPL use the following equation [13]:

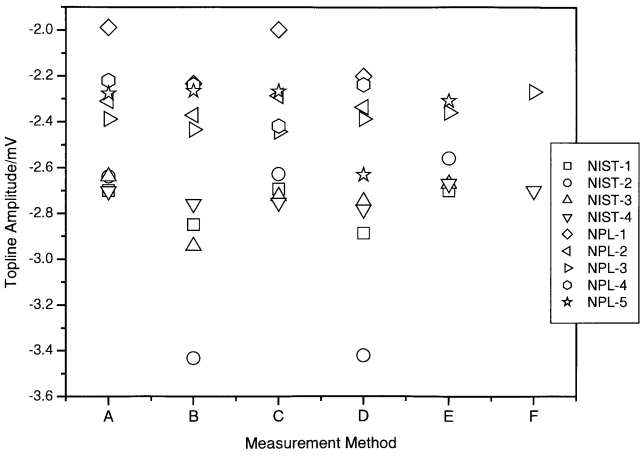

Fig. 7. Topline (S_2) values for the measured waveforms obtained using different pulse parameter measurement methods A to F (explained in Section III-A of the text). The key represents the nine different waveforms for which the pulse parameters were measured. Methods A to D have been applied to all nine waveforms, Method E to six waveforms, and Method F to two waveforms (see explanation in Section III-A).

$$OS = \frac{V_{\max} - S_2}{S_2 - S_1} 100,$$
$$US = \frac{S_1 - V_{\min}}{S_2 - S_1} 100$$

where $V_{\max}$ and $V_{\min}$ are the waveform extrema. For transition duration (see Fig. 4), NIST linearly interpolates between sampling instants to find the reference level instants corresponding to the selected reference levels [13], [15], such as the 10% and 90% reference levels. To find the transition duration, NPL fits a quadratic least squares to five data points (typical) around each reference level and then uses the coefficients of the curve fitted to the data to interpolate the reference level instants. This process reduces the effects of signal noise on the computation of the reference level instant.

The NIST-measured waveforms have longer transition durations than the NPL-measured waveforms (see Fig. 4). The differences shown in Fig. 4 are most likely a consequence of the NIST sampler having a slightly smaller bandwidth than the NPL sampler.

The post-transition overshoot in a waveform is affected by sampler bandwidth and since the NPL sampler exhibited a slightly greater bandwidth than did the NIST sampler used in this comparison, this bandwidth difference may have contributed to the larger observed overshoot in the NPL data compared to the NIST data (see Fig. 5). Noise may also affect the overshoot values since overshoot is defined as the local extremum.

The undershoot observed in the waveforms is more of a low-frequency oscillatory artifact than a peaked artifact and, therefore, is less affected by sampler bandwidth than is the overshoot. Also, undershoot will be sensitive to the position of the transition in the epoch because of the small-amplitude oscillations prior to the transition. The effect of transition position can be

TABLE I
EFFECT OF CORRECTION METHODS ON PULSE PARAMETERS FOR WAVEFORM NIST

	uncorrected	time corrected	gain corrected	time then gain corrected	gain then time corrected
number of points	1024				
top level (V)	-2.69e-03	-2.68e-03	-2.81e-03	-2.81e-03	-2.81e-03
bottom level (V)	-2.46e-01	-2.46e-01	-2.44e-01	-2.44e-01	-2.44e-01
amplitude (V)	2.43e-01	2.43e-01	2.42e-01	2.42e-01	2.42e-01
$t_{10\text{-}90}$ (s)	2.17e-11	2.18e-11	2.17e-11	2.18e-11	2.18e-11
$t_{20\text{-}80}$ (s)	1.48e-11	1.50e-11	1.48e-11	1.50e-11	1.50e-11
overshoot (%)	3.37e+00	3.36e+00	3.37e+00	3.37e+00	3.37e+00
undershoot(%)	2.03e-01	2.27e-01	2.03e-01	2.30e-01	2.30e-01
histogram bins	4084	6849	4084	6770	6770

TABLE II
TRANSITION DURATION(S) OF RECONSTRUCTED WAVEFORMS

Input waveform	NPL results	NIST results	Target value
g1, f1, n0	2.184e-11	2.190e-11	2.175e-11
g1, f1, n1	2.192e-11	2.200e-11	2.175e-11
g1, f1, n2	2.192e-11	2.247e-11	2.175e-11
g1, f2, n0	2.178e-11	2.187e-11	2.175e-11
g1, f2, n1	2.185e-11	2.190e-11	2.175e-11
g1, f2, n2	2.175e-11	2.198e-11	2.175e-11
g1, f3, n0	2.184e-11	2.188e-11	2.175e-11
g1, f3, n1	2.192e-11	2.194e-11	2.175e-11
g1, f3, n2	2.207e-11	2.243e-11	2.175e-11
g1, f4, n0	2.177e-11	2.178e-11	2.175e-11
g1, f4, n1	2.189e-11	2.184e-11	2.175e-11
g1, f4, n2	2.203e-11	2.204e-11	2.175e-11
g1, f5, n0	2.177e-11	2.174e-11	2.175e-11
g1, f5, n1	2.180e-11	2.178e-11	2.175e-11
g1, f5, n2	2.185e-11	2.193e-11	2.175e-11
g2, f1, n0	2.777e-11	2.782e-11	2.810e-11
g2, f1, n1	2.790e-11	2.774e-11	2.810e-11
g2, f1, n2	2.715e-11	2.717e-11	2.810e-11
g2, f2, n0	2.774e-11	2.777e-11	2.810e-11
g2, f2, n1	2.776e-11	2.776e-11	2.810e-11
g2, f2, n2	2.792e-11	2.763e-11	2.810e-11
g2, f3, n0	2.792e-11	2.783e-11	2.810e-11
g2, f3, n1	2.809e-11	2.786e-11	2.810e-11
g2, f3, n2	2.729e-11	2.728e-11	2.810e-11
g2, f4, n0	2.772e-11	2.786e-11	2.810e-11
g2, f4, n1	2.768e-11	2.779e-11	2.810e-11
g2, f4, n2	2.788e-11	2.770e-11	2.810e-11
g2, f5, n0	2.773e-11	2.805e-11	2.810e-11
g2, f5, n1	2.777e-11	2.804e-11	2.810e-11
g2, f5, n2	2.786e-11	2.797e-11	2.810e-11
μ_{error}	1.167e-13	6.586e-14	
σ_{error}	3.008e-13	3.666e-13	

seen in Fig. 6 by comparing Methods A and B and Methods C and D (B and D are the truncated waveforms) for the NIST waveforms. Noise may also affect the undershoot values since undershoot is defined as the local extremum.

1) Recommendations: For reproducibility and accurate comparisons of pulse parameter values, it is important that waveforms having the same waveform epoch and transition position be used. For the work presented in this section, the same waveform epoch was used but not necessarily the same relative transition position (see Fig. 2). However, by truncating the waveforms, it was possible to simulate waveforms with the same transition position. Comparing the raw (or measured)

TABLE III
OVERSHOOT (PERCENT OF PULSE AMPLITUDE) OF RECONSTRUCTED WAVEFORMS

Input waveform	NPL results	NIST results	Target value
g1, f1, n0	3.34	3.26	3.258
g1, f1, n1	3.63	3.41	3.258
g1, f1, n2	3.93	3.45	3.258
g1, f2, n0	3.26	3.15	3.258
g1, f2, n1	3.31	3.15	3.258
g1, f2, n2	3.26	3.59	3.258
g1, f3, n0	3.31	3.28	3.258
g1, f3, n1	3.74	3.42	3.258
g1, f3, n2	3.75	3.56	3.258
g1, f4, n0	3.26	3.28	3.258
g1, f4, n1	3.58	3.31	3.258
g1, f4, n2	3.61	3.21	3.258
g1, f5, n0	3.26	3.28	3.258
g1, f5, n1	3.23	3.26	3.258
g1, f5, n2	3.28	3.21	3.258
g2, f1, n0	10.26	10.05	10.436
g2, f1, n1	9.93	10.05	10.436
g2, f1, n2	10.76	9.73	10.436
g2, f2, n0	11.19	10.23	10.436
g2, f2, n1	11.11	10.17	10.436
g2, f2, n2	10.87	9.68	10.436
g2, f3, n0	10.83	10.05	10.436
g2, f3, n1	10.62	10.08	10.436
g2, f3, n2	10.41	9.48	10.436
g2, f4, n0	10.98	10.83	10.436
g2, f4, n1	11.01	10.80	10.436
g2, f4, n2	10.72	10.29	10.436
g2, f5, n0	11.01	10.98	10.436
g2, f5, n1	10.86	10.92	10.436
g2, f5, n2	10.91	10.37	10.436
μ_{error}	-0.260	0.063	
σ_{error}	0.294	0.358	

data is a useful exercise because it will provide a clue as to the origin of differences, if they exist, between reported pulse parameter values.

B. Corrected Waveforms

NPL does not usually correct their measured waveforms for sampler gain or time-base errors because typically these errors are small and their effects are included with the uncertainty contributions. These errors are typically small compared to the overall parameter uncertainty. When these errors are significant, NPL does correct the waveforms. NIST does correct their waveforms, and an example of the effect of the correction is shown in Table I for NIST measured waveform NIST-1. The order of time and gain correction was exchanged to verify that corrections were linear to the desired precision for the amount of correction required (see columns 5 and 6 of Table I).

The number of bins found in the optimal search routine [14] exceeds that expected by the effective number of bits because of waveform averaging: each acquired waveform was the result of at least 1024 internally-averaged (by the sampler) waveforms.

Recommendations. It is apparent from Table I that the effect of waveform correction is well below the uncertainty reported to the customer. Consequently, applying a correction algorithm may not always provide additional benefit to the customer in terms of reduced uncertainty. However, if a bias in a pulse parameter does exist because of a known error, then that parameter's uncertainty estimate is no longer symmetric. That is, the error introduces a bias in the uncertainty. Time-base errors can be large and nonlinear with time, resulting in a contraction/expansion of several picoseconds over an entire 2-ns epoch [17]–[19]. However, if the time-base errors are applied locally to the transition region of the waveform and the waveform is positioned within a region of the epoch that exhibits a nominally

TABLE IV
UNDERSHOOT (PERCENT OF PULSE AMPLITUDE) OF RECONSTRUCTED WAVEFORMS

Input waveform	NPL results	NIST results	Target value
g1, f1, n0	0.25	0.20	0.202
g1, f1, n1	0.23	0.10	0.202
g1, f1, n2	0.59	0.51	0.202
g1, f2, n0	0.23	0.23	0.202
g1, f2, n1	0.23	0.23	0.202
g1, f2, n2	0.20	0.03	0.202
g1, f3, n0	0.23	0.20	0.202
g1, f3, n1	0.41	0.23	0.202
g1, f3, n2	0.87	0.56	0.202
g1, f4, n0	0.23	0.20	0.202
g1, f4, n1	0.38	0.20	0.202
g1, f4, n2	0.48	0.25	0.202
g1, f5, n0	0.23	0.20	0.202
g1, f5, n1	0.20	0.20	0.202
g1, f5, n2	0.20	0.18	0.202
g2, f1, n0	1.17	1.17	1.172
g2, f1, n1	1.19	1.25	1.172
g2, f1, n2	1.42	1.30	1.172
g2, f2, n0	1.18	1.20	1.172
g2, f2, n1	1.21	1.20	1.172
g2, f2, n2	1.29	1.36	1.172
g2, f3, n0	1.18	1.17	1.172
g2, f3, n1	1.23	1.22	1.172
g2, f3, n2	1.23	1.19	1.172
g2, f4, n0	1.18	1.18	1.172
g2, f4, n1	1.18	1.18	1.172
g2, f4, n2	1.26	1.23	1.172
g2, f5, n0	1.18	1.18	1.172
g2, f5, n1	1.20	1.18	1.172
g2, f5, n2	1.09	1.12	1.172
μ_{error}	-0.085	-0.035	
σ_{error}	0.149	0.102	

linear error [20], then the uncertainty in the transition duration will be symmetric.

C. Reconstruction Comparison Using Simulated Waveforms

The measured or acquired waveforms can be described as the convolution of the input pulse with the sampler impulse response and the jitter. To perform the comparison of reconstructed waveforms, the effect of reconstruction algorithm and sampler impulse response estimate has to be separated. NIST and NPL use different "blind" reconstruction algorithms, that is, reconstruction algorithms where no *a priori* information on the impulse response is used or required. The "measured" waveforms were simulated by convolving sampler impulse response estimates with already-measured waveforms (which are the target or simulated input waveforms). The effect of noise on the reconstruction process was also investigated by adding different levels of noise to the "measured" waveforms.

In Tables II–IV, the input waveform is the result of the convolution of an input signal with a filter after which noise is added. The input signals are g1 (3-dB attenuation bandwidth, $\mathrm{BW}_{3\mathrm{db}}, \cong$ 20 GHz) and g2 ($\mathrm{BW}_{3\mathrm{db}} \cong$ 16 GHz), which are the measured output of two different pulse generators, the filters are given by f1 to f5, and the added noise is represented by n0 to n2. Filters f1 and f2 are second-order filters with 3-dB attenuation bandwidths of approximately 16 GHz and 20 GHz. Filters f3 to f5 are Gaussian filters with decreasing bandwidths of approximately 50 GHz, 20 GHz, and 12 GHz. The noise that was added is 0 V rms for n0, 100 μV rms for n1, and 1 mV rms for n2. The target values for the pulse parameters are those of g1 and g2. The nominal pulse amplitude of g1 and g2 is 1 V. The impulse responses of the filters integrate to one and, consequently,

do not cause the amplitude of the input waveform to differ from that of the target (or input) signal.

Tables II–IV show that the differences between pulse parameters obtained using the NIST and NPL waveform reconstruction methods are small. Both reconstruction methods are affected by noise and filter type to about the same magnitude. In Tables II–IV, columns 2 and 3 represent the pulse parameter values of the NPL (column 2) and NIST (column 3) reconstructed waveforms using the NIST pulse parameter software for 2^n histogram bins. For comparison, column 4 represents the target values (parameters of the unfiltered signals, either g1 or g2) calculated using the NIST pulse parameter software. The reason one source of software is used in this part of the comparison is to avoid introducing any differences in the extracted pulse parameters of the reconstructed waveforms that may have been caused by the differences between the NIST and NPL pulse parameter algorithms. The average error, given by μ_{error}, represents the bias in the pulse parameter values caused by the waveform reconstruction process. The σ_{error} is the sample standard deviation.

Recommendations The data in Tables II–IV show that both reconstruction methods work well. The errors in the pulse parameter values show that the reconstruction method imposes a bias on those parameters. The only parameter for which both NIST and NPL have a published uncertainty [1], [2] is transition duration. For transition duration, the bias is less than one-tenth of the published uncertainty and standard deviation is less than one-fifth of the published uncertainty.

IV. Conclusion

A comparison of the pulse measurement services from NPL and NIST shows that the pulse parameter values for both national laboratories are within published uncertainties. For transition duration, the difference between NPL and NIST values are within the published uncertainties [1], [2] and these differences are dominated by the different impulse responses of the samplers used and, perhaps the uncertainty in the sampler impulse response estimate. For undershoot/preshoot, the primary differences between NPL and NIST are due to the different sampler impulse responses and their estimates. The differences observed between the overshoot values determined by NPL and NIST are equally affected by the reconstruction process and the different samplers used. For amplitude, the differences between the values reported by NPL and NIST are dominated by the different sampler responses; however, these differences are within the published uncertainties.

Acknowledgment

The authors would like to thank B.C. Waltrip and B.A. Bell of NIST-Gaithersburg, D.C. DeGroot of NIST-Boulder, and D. Ives of NPL for technical comments.

References

[1] *NIST Calibration Services Users Guide*, U.S. Department of Commerce, Washington, DC, Jan. 1998, pp. 189–193.

[2] *http://www.npl.co.uk/npl/cem/ufe-opto/calibration/ufe-calibration.html* [Online]

[3] N. S. Nahman and M. E. Guillaume, Deconvolution of Time Domain Waveforms in the Presence of Noise, U.S. Department of Commerce, Washington, DC, 1981.

[4] N. G. Paulter, "A causal regularizing deconvolution filter for optimal waveform reconstruction," *IEEE Trans. Instrum. Meas.*, vol. 43, pp. 740–747, Oct. 1994.

[5] T. Daboczi, "Uncertainty of signal reconstruction in the case of jittery and noisy measurements," *IEEE Trans. Instrum. Meas.*, vol. 47, pp. 1062–1066, Oct. 1998.

[6] A. J. A. Smith, A. G. Roddie, and D. Henderson, "Electrooptic sampling of low temperature GaAs pulse generators for oscilloscope calibration," *Opt. Quant. Electron.*, vol. 28, pp. 933–944, 1996.

[7] P. D. Hale, T. S. Clement, K. J. Coakley, C. M. Wang, D. C. DeGroot, and A. P. Verdoni, "Estimating the magnitude and phase response of a 50 GHz sampling oscilloscope using the 'nose-to-nose' method," in *Automatic Radio Frequency Techniques Group, 55th ARFTG Conf. Dig.*, Boston, MA, June 2000.

[8] D. Henderson, A. G. Roddie, and A. J. A. Smith, "Recent developments in the calibration of fast sampling oscilloscopes," *Proc. Inst. Elect. Eng. A*, vol. 139, pp. 254–260, Sept. 1992.

[9] A. J. A. Smith, A. G. Roddie, and P. D. Woolliams, "Electro-optic sampling of coplanar to coaxial transitions to enhance the calibration of fast oscilloscopes," in *Automatic Radio Frequency Techniques Group, 55th ARFTG Conf. Dig.*, Boston, MA, June 2000.

[10] A. J. A. Smith, A. G. Roddie, P. D. Woolliams, and M. R. Harper, "Aberration measurement of fast pulse generators using sampling oscilloscopes," in *Automatic Radio Frequency Techniques Group, 55th ARFTG Conf. Dig.*, Boston, MA, June 2000.

[11] N. G. Paulter, "Low-jitter trigger system for pulse calibration and comparison of high-speed samplers," *IEEE Trans. Instrum. Meas.*, vol. 47, pp. 606–608, June 1998.

[12] Pulse Techniques and Apparatus, Part 2: Pulse Measurement and Analysis, General Considerations, 2nd ed., 1987.

[13] IEEE Subcommittee on Pulse Techniques*http://grouper.ieee.org/groups/181/index.html* [Online]

[14] N. G. Paulter, "The effect of histogram size on histogram-derived pulse parameters," *IEEE Trans. Instrum. Meas.*, vol. 47, pp. 609–612, June 1998.

[15] Pulse Techniques and Apparatus, Part 1: Pulse Terms and Definitions, 2nd ed., 1987.

[16] D. R. Larson and N. G. Paulter, "Temperature effects on the high speed response of digitizing sampling oscilloscopes," in *NCSL Int. Workshop Symp.*, Toronto, ON, Canada, July 16–20, 2000.

[17] G. N. Stenbakken and J. P. Deyst, "Time-base nonlinearity determination using iterated sine-fit analysis," *IEEE Trans. Instrum. Meas.*, vol. 47, pp. 1056–1061, Oct. 1998.

[18] C. M. Wang, P. D. Hale, and K. J. Coakley, "Least-squares estimation of time-base distortion of sampling oscilloscopes," *IEEE Trans. Instrum. Meas.*, vol. 48, pp. 1324–1332, Dec. 1999.

[19] J. Verspecht, "Accurate spectral estimation based on measurements with a distorted-timebase digitizer," *IEEE Trans. Instrum. Meas.*, vol. 43, pp. 210–215, Apr. 1994.

[20] N. G. Paulter and D. R. Larson, "Time-base setting dependence of pulse parameters using high-bandwidth digital sampling oscilloscopes," in *NCSL Int. Workshop and Symp.*, Toronto, ON, Canada, July 16–20, 2000.

N. G. Paulter received the M.S. degree in chemistry from the University of New Mexico, Albuquerque, in 1988 and the M.S. degree in electrical engineering from the University of Colorado, Boulder, in 1990.

He was with Los Alamos National Laboratory, Los Alamos, NM, from 1980 to 1989, and was involved in the study of fast electrical phenomena and in the development of high-speed photoconductors for use as ultrafast light detectors and sampling gates. In 1989, he joined the National Institute of Standards and Technology (NIST), Boulder, to develop transient pulse measurement techniques and analysis. He is presently with NIST, Gaithersburg, MD. His present research interests include semiconductor physics, materials properties, electrooptics, ultrafast electronic phenomena, and waveform/data processing and analysis.

Andrew J. A. Smith received the B.Sc. degree (First Class Honors) from Loughborough University of Technology and the Ph.D. degree in fast waveform metrology from UCL, London, U.K., in 1995.

He joined the National Physical Laboratory (NPL), U.K., in 1989. His primary research focuses on femtosecond photoconductive pulse generator and electrooptic sampling for metrology applications. His recent work includes real-time instrumentation, jitter analysis, and high-voltage digitisers. He is also the Manager of the NPL risetime calibration facility. He has written 18 conference and journal papers

Dr. Smith is a Member of the Institute of Physics and a Chartered Physicist. He was awarded the IEE's Duddell Premium in 1993.

D. R. Larson (M'79–SM'94) received the B.S. degree (*cum laude*) from Brigham Young University, Provo, UT, in 1978 and the M.S.E.E. degree from the University of Colorado, Boulder, in 1981.

He was with the Optoelectronics Division, National Institute of Standards and Technology (NIST), Boulder, from 1976 until 1998. He has been with the Electricity Division, NIST, Gaithersburg, MD, since 1998.

T. M. Souders, photograph and biography not available at the time of publication.

Alan G. Roddie received the degree in physics from the University of St. Andrews, U.K., in 1969 and the Ph.D. degree for investigation of picosecond dye lasers from the Queen's University, Belfast, U.K. in 1972.

He led the Ultrafast Electrical Measurement Group at the National Physical Laboratory (NPL), U.K., for over 18 years, extending the use of sophisticated state-of-the-art techniques in optoclectronics to provide traceable calibration services. He now operates a consultancy in the metrology of fast electrical signals and laser power.